chemengineering

MDPI

Article

Synthesis of Uniform Mesoporous Zeolite ZSM-5 Catalyst for Friedel-Crafts Acylation

Heman A. Smail [1], Mohammad Rehan [2], Kafia M. Shareef [3], Zainab Ramli [4], Abdul-Sattar Nizami [2] and Jabbar Gardy [1,5,*]

1 Department of Chemistry, College of Science, Salahadin University-Hawler, Erbil 44002, Kurdistan Region, Iraq; heman.smail@su.edu.krd
2 Center of Excellence in Environmental Studies, King Abdulaziz University, Jeddah 21589, Saudi Arabia; dr.mohammad_rehan@yahoo.co.uk (M.R.); nizami_pk@yahoo.com (A.-S.N.)
3 Department of Nursing, Ishik University, 100 Meter Campus, Erbil 44001, Kurdistan Region, Iraq; kafia.mawlood@ishik.edu.iq
4 Departments of Chemistry, College of Science, Universiti Technologi Malaysia (UTM), UTM Skudai 81310, Johor, Malaysia; zainab@kimia.fs.utm.my
5 School of Chemical and Process Engineering (SCAPE), University of Leeds, Leeds LS2 9JT, UK
* Correspondence: jabbar.gardy@su.edu.krd or j.gardy@leeds.ac.uk; Tel.: +96-4750-7608-855

Received: 4 March 2019; Accepted: 31 March 2019; Published: 4 April 2019

Abstract: This work highlights how the treatment of ZSM-5 (parent Zeolite Socony Mobil–5, Si/Al = 23) with different surfactant templates and alkaline solution, improved the catalytic performance in the Friedel-Crafts acylation of anisole with a propionic anhydride to obtain p-methoxypropiophenone. The modified microporous to mesoporous zeolite catalysts were characterized using different analytical techniques, including X-ray diffraction (XRD), nitrogen porosimetry, Fourier-transform infrared spectroscopy (FT-IR), temperature-programmed desorption (ammonia-TPD) and field emission scanning electron microscopy (FE-SEM) to analyze the crystallographic structure, surface acidity, surface area, porosity, morphology, and particle size. The results showed that the formed mesoporous zeolite by NaOH solution had smaller mesopores (ca. 3.7 nm) as compared to the mesoporous zeolites obtained by surfactant templates, such as, CTAB (ca. 14.9 nm), TPAOH (ca. 11.1 nm) and mixture of CTAB/TPAOH (ca. 15.2 nm). The catalytic acylation reaction was conducted in a batch glass reactor at various temperatures and the products were analyzed using off-line gas chromatography–mass spectrometry (GC-MS). It was found that the activity of treated ZSM-5 with mixed surfactant templates (CTAB/TPAOH) exhibited enhanced selectivity towards the main product (p-methoxypropiophenone) by a factor 1.7 or higher than unmodified ZSM-5 due to its increased surface area by 1.5 times and enhanced acid sites.

Keywords: ZSM-5; mesoporous zeolite; Friedel-Crafts acylation; modification of ZSM-5; anisole

1. Introduction

The Friedel-Crafts acylation is one of the most vital organic reactions in the preparation of substituted aromatic ketones in pharmaceutical, fragrance, cosmetics and agrochemical industries. Catalysts such as strong mineral acids (H_2SO_4 and HF) and metal halides (and $FeCl_3$ and $AlCl_3$) have been used in the conventional acylation method [1]. The overall process produces a high amount of hazardous waste which is difficult to separate from the product. Because of the disadvantages, the use of recyclable and environment-friendly solid acid catalysts, such as zeolite, is desirable. This is to minimize economic and environmental problems [2]. Zeolite can be used as a catalyst in the Friedel-Crafts acylation reaction. The electrophilic acylation of anisole (methoxybenzene) with phenyl

acetate, phenyl acetyl chloride, phenyl propionic, phenylpropionyl chloride [3], acetyl chloride [4] and acetic anhydride [5–7] has been widely reported. The catalyst activity and selectivity of zeolite H-Beta, H-ZSM-5, H-Y, and NH_4-Y catalysts in the acylation reaction of anisole with acetic anhydride were compared by Freese et al. [5]. They reported a lower catalytic activity of H-ZSM-5 compared to H-Y and H-Beta catalysts with only 14% of conversion; this is due to smaller intersection channels in ZSM-5 [8].

Zeolites are microporous crystalline aluminosilicates that have a similar composition to the clay minerals. However, they are different in their well-defined three-dimensional microporous structures. Silicon, aluminum, and oxygen are arranged in a regular structure of tetrahedral units of $[SiO_4]^-$ and $[AlO_4]^-$, forming a framework with regular pores. The pores are in the form of channels, tunnels, or cavities with a diameter of around 0.1–2 nm running through the material [9].

Mesoporous zeolites, consisting of microporous structure and intra-crystalline mesoporosity, show improved catalytic activities in many organic reactions because of their enhanced reactants and products diffusion from/to active sites in microporous via the mesoporous frameworks [10]. Such materials help to overcome the limitation of microporous zeolites pore size and therefore allow large molecules to diffuse through [11]. The synthesis of mesoporous ZSM-5 via a dissolution process include the re-assembling of amorphous silica directed by surfactant molecules simultaneously; the re-assembling of the total dissolved structure of zeolite around surfactant molecules has also been reported [12]. In the presence of long-chain alkyl ammonium surfactants, the dissolved silicates accumulate within surfactant molecules to make micelles and re-precipitate onto the surface of parent spheres surface to convert amorphous silica into mesoporous silica during the hydrothermal reaction [13].

The synthesis of mesoporous ZSM-5 zeolites has been extensively studied using a silylated polyethylenimine as a mesoporous-directing agent and polymers are the most widely used templates, including long-chain organosilicates, amphiphilic surfactants [14], polyvinyl butyral [15], CTAB, F127, and P123 [16]. The lesser reactive Al sites support the maintenance of the zeolite framework in an alkaline medium, while the Si atoms dissolve, rendering more open structures. Desilication in comparison to dealumination provides more controllable mesoporosity and also preserves the Brønsted acidity [17]. The study of ZSM-5 and silicalite-treated alkali with sodium hydroxide aqueous solutions at high concentrations showed that Si atoms could be removed with no change in the crystallinity of the zeolites. Therefore, the present work is focused on the synthesis of ZSM-5 and the treatment of synthesized zeolite with an alkali solution as well as several different surfactant templates to form a uniform-sized mesoporous material without deterioration of crystallinity of the parent zeolite structure. The catalytic activity of untreated and treated zeolite catalysts was also studied in a batch reactor at different temperatures.

2. Material and Methods

2.1. Materials

Cetyl trimethyl ammonium bromide (CTAB) was purchased from Fisher Scientific whilst tetra propyl ammonium hydroxide (TPAOH), sodium hydroxide (NaOH), ammonium nitrate (NH_4NO_3), anisole and propionic anhydride were obtained from Merck. NH_4-ZSM-5 (Si/Al = 23) was purchased from Zeolyst International.

2.2. Synthesis of Mesoporous ZSM-5 Catalyst

NH_4-ZSM-5 zeolite (0.176 g) was dispersed in deionized water (20 g) using an ultrasonic bath. TPAOH (0.2 g) was separately dissolved in a solution consisting of NaOH (0.312 g) and deionized water (20 g). The prepared solution was appropriately mixed using an ultrasonic bath for 5 min and then put in a Teflon-lined autoclave. The hydrothermal treatment of the obtained solution was performed at 100 °C for 24 h. Further, the treated product was washed a few times using deionized

water followed by vacuum filtration. Afterward, the collected wet sample was oven-dried at 80 °C overnight. This sample was then calcined up to 550 °C with a 1 °C·min^{-1} heating rate and oxygen as a purge gas followed by maintaining the temperature of 550 °C for a period of 6 h to allow the removal of the remaining surfactant template. The same procedure was repeated for other surfactant templates (CTAB and mixed CTAB and TPAOH) and alkaline solution (NaOH) treatments. Finally, the dried catalysts were labeled, as listed in Table 1.

Table 1. Zeolite catalyst coding.

Catalysts	Label Code
Untreated zeolite catalyst	ZSM-5
Treated zeolite with NaOH	ZSM-5-Na
Treated zeolite with CTAB	ZSM-5-C
Treated zeolite with TPAOH	ZSM-5-T
Treated zeolite with mixed CTAB and TPAOH	ZSM-5-CT

2.3. Characterization Methods

2.3.1. X-Ray Diffraction (XRD)

The crystal structure of all prepared zeolite catalysts was identified at room temperature by XRD (Siemens D5000 diffractometer, Siemens AG, Munich, Germany) using Bragg-Brentano geometry, λ = 0.1541 nm CuKα radiation at 40 kV, and a current of 30 mA. Each powder catalyst was loaded onto the sample holder and scanned at 2θ angle range from 5–50° with a 0.05° angular step size [18]. The average crystallite size of zeolite catalysts was calculated according to the Debye-Scherrer's formula (see Equation (1)) [19] while the crystallinity was calculated [20] using Equation (2).

$$\text{Crystallite size (D)} = k\lambda/\beta\cos\theta \quad (1)$$

where k is a shape factor of the particles (k = 0.9), λ is a wavelength of the CuKα radiation, θ is the incident angle of the X-rays, and β is the full width at half maxima of the diffraction peaks (FWHM).

$$\text{Crystallinity\%} = \frac{\Sigma\text{Intensity of peaks of catalyst}}{\Sigma\text{Intensity of peaks of standard}} \times 100 \quad (2)$$

2.3.2. Fourier Transform Infrared (FT-IR) Spectroscopy

The functional groups present in the untreated zeolite (parent ZSM-5) and treated zeolite catalysts were examined by FT-IR spectrometer (Perkin Elmer Spectrum One, PerkinElmer, Waltham, MA, USA) at room temperature. At least 36 scans were conducted using an average infrared signal with a resolution of 4 cm^{-1} within the range of 400–4000 cm^{-1} and the final output was in transmittance%. The samples were made ready by mixing 5 mg of each zeolite catalyst on 200 mg of KBr pressed into a disk for FT-IR measurement.

2.3.3. Nitrogen Porosimetry

The surface area of untreated and treated ZSM-5 catalysts was obtained according to the Brunauer-Emmer-Teller (BET) method using multipoint N_2 adsorption-desorption at 77.3 K employing Micromeritics (3FLEX surface characterization) analyzer (Micromeritics Instrument Corporation, Norcross, GA, USA). All catalysts had been pre-treated at 350 °C for 4 h under a vacuum to dehydrate the catalysts prior to analysis. In order to calculate the BET surface area, the N_2 adsorption isotherms ($\Delta G_{ads.} = RT(\ln P_{ads.} - \ln P_o)$) data over the relative pressure range of 0.05–0.3 were used for all catalyst samples. However, desorption isotherms ($\Delta G_{des.} = RT(\ln P_{des.} - \ln P_o)$) were used to calculate the average pore size and total pore volume for all samples using the Barrett-Joyner-Halenda (BJH) method. Since $P_{des.} < P_{ads.}$ it follows that $\Delta G_{des.} < \Delta G_{ads.}$. Hence, the desorption value of relative

pressure corresponds to the more stable adsorbate condition and that is why desorption isotherms should be used for pore size analysis [21].

2.3.4. Morphology

The sizes and morphological features of the zeolite catalysts were examined employing a field emission scanning electron microscope (FE-SEM, ZEISS SIGMA, Zaventem, Belgium). A few particles of each untreated and treated ZSM-5 catalyst were separately dispersed in acetone then one drop of the suspended catalyst was put on a sample holder and coated with Pt before analysis to remove the charging effect from the electron beam.

2.3.5. Surface Acidity

The temperature programmed desorption-ammonia (NH_3-TPD) analysis was conducted by a Micromeritics Auto Chem II analyzer (TPD/TPR, Micromeritics, Norcross, GA, USA) using a thermal conductivity detector (TCD, Thermo Scientific, Mainz, Germany). The zeolite catalyst (0.04 g) was heated to 560 °C under helium purge gas at 30 mL·min^{-1} before carrying out the measurement. The sample was first cooled down to 180 °C, and then the ammonia adsorption was conducted for 30 min using an ammonia flow rate of 30 mL·min^{-1}. The catalyst was purged with helium (30 mL·min^{-1}) for 90 min to eliminate un-reacted ammonia on the surface of the catalyst before NH_3-TPD measurements. The NH_3-TPD measurements of the catalysts were performed by increasing the temperature from 180 to 550 °C at 15 °C·min^{-1} heating rate under 30 mL·min^{-1} of helium purge gas. Once the temperature reached 550 °C, the catalyst was held for 30 min.

2.4. Synthesis of p-Methoxypropiophenone "Friedel-Crafts Acylation"

Ion exchange for all treated zeolite catalysts was performed before their catalytic performances as follows: 1.0 g of each modified zeolite catalysts was separately stirred in 20 mL of 1.0 M NH_4NO_3 aqueous solution at 60 °C for 6 h. These catalysts were then filtered, washed few times using deionized water, and oven-dried at 60 °C overnight followed by calcination at 500 °C for 3 h to obtain the final H^+ type ZSM-5 (or NH_4-ZSM-5). Then, 0.5 g of untreated NH_4-ZSM-5 and the treated catalyst was activated at a temperature of 500 °C for 3 h in the air before the reaction. 30 mmol of anisole and 30 mmol of propionic anhydride were gently stirred under N_2 gas for 10 min. The obtained solution was then poured to a 100 mL batch glass vessel reactor containing the activated catalyst. Afterward, the solution was heated at the temperature of 100 °C under reflux and a N_2 atmosphere, and vigorously stirred for 24 h. The final product was separated from the catalyst particles by centrifugation for 15 min, and a few mL of the product was then analyzed by off-line GC-MS (gas chromatography equipped with a mass spectroscopy) as follows: Initially, 1.0 µL of the catalyst was injected into the GC at 50 °C for 1 min before increasing the temperature to 200 °C at 8 °C·min^{-1} rate, after which the temperature was maintained for 35 min. The same procedure was repeated for catalytic reactions performance at different temperatures and all other treated zeolite catalyst with ZSM-5-Na, ZSM-5-C, ZSM-5-T, and ZSM-5-CT. The separated spent catalyst particles were washed repeatedly with deionized water and then calcined for 3 h at 500 °C for further investigations in order to assess the catalyst lifetime. The detailed investigations will be reported in the future studies.

3. Results and Discussion

3.1. Zeolite Catalyst Characterizations

XRD was used to analyze the crystal structures of untreated and treated zeolite catalysts. The diffraction patterns of all treated zeolite catalysts were similar compared to the untreated zeolite (parent ZSM-5), and all diffraction peaks matched with that of H-ZSM-5 (JCPDS 44-0003). However, the peak intensities of treated zeolite catalysts were slightly reduced, though without any destruction in the framework. Figure 1 shows that some silicon atoms were removed from the framework by

decreasing the ratio of Si/Al appearing at 2θ from 5 to 20°. Table 2 presents the crystallite size and amount of crystallinity for the treated and untreated zeolite catalysts.

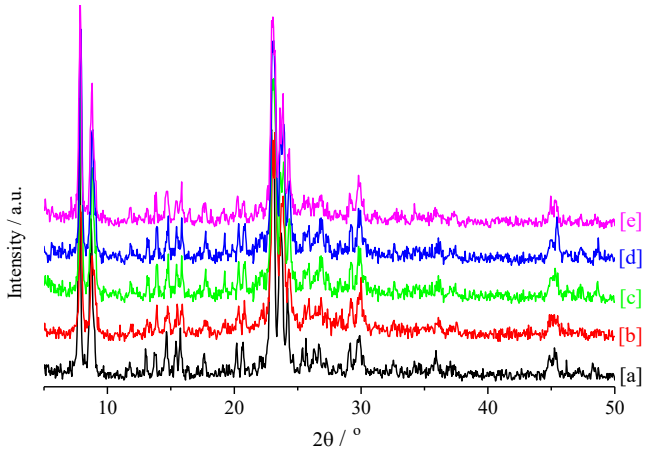

Figure 1. XRD patterns for (**a**) ZSM-5, (**b**) ZSM-5-Na, (**c**) ZSM-5-C, (**d**) ZSM-5-T and (**e**) ZSM-5-CT.

Table 2. The crystallite size and crystallinity of treated and untreated zeolite catalysts.

Catalysts	Crystallite Size (nm)	Crystallinity (%)
ZSM-5	22	100
ZSM-5-Na	21	86
ZSM-5-C	21	93
ZSM-5-T	20	93
ZSM-5-CT	21	95

Figure 2a,b presents the FT-IR spectra before and after ion exchange, respectively, for all untreated and treated zeolite catalysts. The absorption band located at 3636 cm^{-1} was attributed to the O–H stretching modes in Si–O–H and/or O–H groups on the surface of the zeolite catalysts [22]. The broad weak band around 3475 cm^{-1} was assigned to the stretching vibration of the O–H bond in silanol groups (Si–O–H) but could be due to the adsorbed water (H–O–H) molecules on the surface of silica. The band at 3142 cm^{-1} was assigned to the stretching vibration of the hydroxyl (O–H) group of water molecules and amines (N–H) present in the pores of the zeolites [22]; bands at 1639 cm^{-1} were attributed to the O–H bending vibration of water molecules [23]. The band at 1400 cm^{-1} in untreated zeolite may be affected by characteristics peak of NH_4^+ and a similar band has been observed for treated zeolites after the ion exchange process [24]. Bands at 1227 and within the range of 1070 to 1150 cm^{-1} were referred to the external asymmetric stretch and the internal asymmetric stretch of T–O–T, respectively. The band at 793 cm^{-1} corresponded to the external symmetric stretch of T–O–T, and that at 455 cm^{-1} was due to the T–O bend (where T = Si or Al) which is typically for the 5-fold rings of highly siliceous materials, whereas the framework vibration around 550 cm^{-1} (double rings) is characteristic of MFI-type zeolites [25].

The surface area, pore sizes, and pore volumes for all untreated and treated zeolite catalysts were determined using N_2 adsorption-desorption isotherms. Figure 3a(i) illustrates the untreated ZSM-5 exhibits Type I adsorption isotherm, while Figure 3a(iii) ZSM-5-Na displays Type IV adsorption isotherm with a hysteresis loop type H3 of plate-like particles, which gives rise to the slit-shaped pores. A hysteresis loop was seen during the desorption measurements in the case of ZSM-5-Na, strongly suggesting the formation of mesoporous ZSM-5 in comparison to the other materials reported mesoporous materials [26]. Furthermore, the synthesized ZSM-5-T can be classified as Type IV with a hysteresis loop type H_2 that is associated with a capillary condensation in the bottle-pore shape. On the other hand, the synthesized catalysts ZSM5-CT and ZSM-5-C were found to be Type VI with a hysteresis loop type H_2. The Type VI isotherm is associated with multilayer adsorption isotherms.

It can be seen from the isotherm in Figure 3a(iv,v) that there were two steps with increased volume which occurred at the P/P_o values of 0.2 and 0.4. Figure 3b(ii,iv,v) show that ZSM-5-C has an average pore size of ca. 14.9 nm whereas ZSM-5-T and ZSM-5-CT have ca.11.1 and 15.2 nm average pore sizes, respectively. The mesoporous structure is present throughout the zeolite catalyst and forms a highly interpenetrating and uniform porous network. In contrast, the isotherm of the untreated zeolite catalyst is typical of microporous materials having high adsorption at low relative pressures.

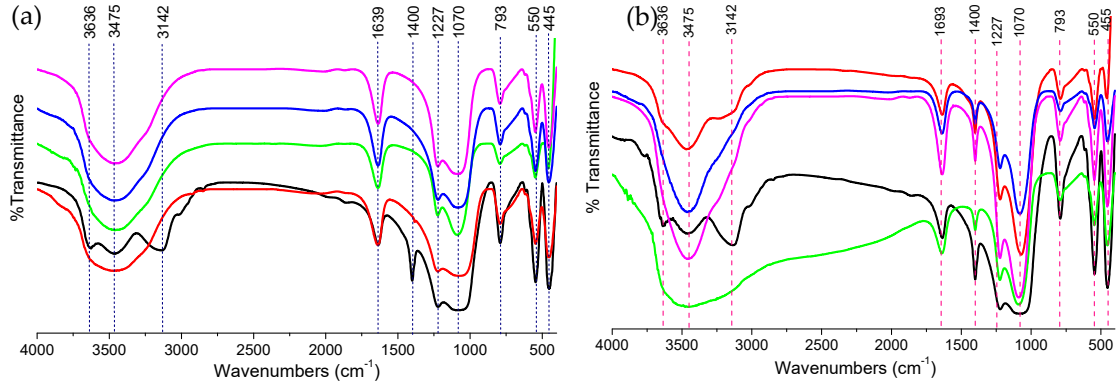

Figure 2. FT-IR spectra for untreated and treated zeolite catalysts before (**a**) and after ion exchange (**b**). Where ZSM-5 is in black, ZSM-5-Na is in red, ZSM-5-C is in green, ZSM-5-T is in blue, and ZSM-5-CT is in purple.

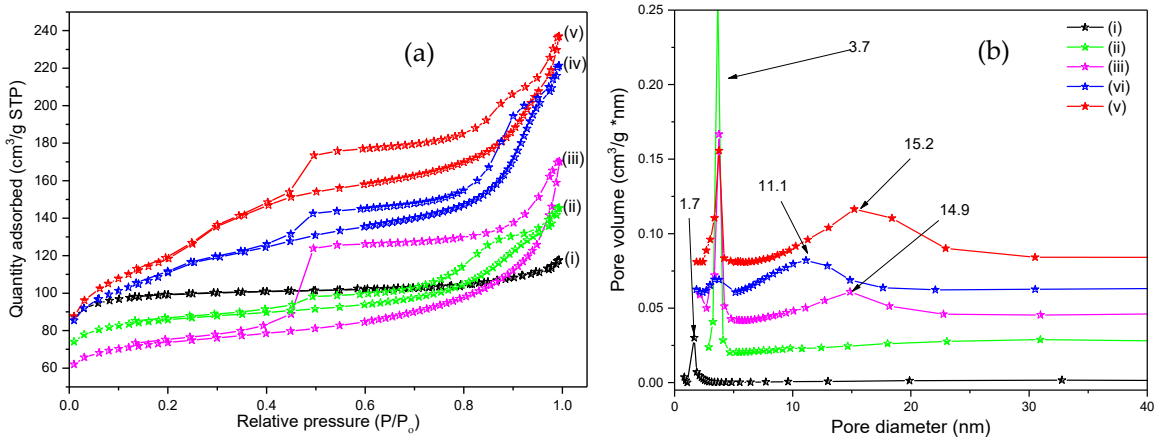

Figure 3. (**a**) N_2 adsorption-desorption isotherm and (**b**) average pore size distribution. (i) ZSM-5, (ii) ZSM-5-T, (iii) ZSM-5-Na, (iv) ZSM-5-CT, and (v) ZSM-5-C.

Table 3 summarizes the BET surface area, average pore size, and total pore volumes result for the treated and untreated zeolite catalysts. It is obvious that the surface area, pore sizes, and volumes of all the treated zeolite catalysts were significantly increased as compared to those of the untreated zeolite catalyst. This is very important for the enhanced catalytic activity of synthesized catalysts. The highest surface area of 419 ± 2.0 $m^2 \cdot g^{-1}$ was received for synthesised ZSM5-CT catalyst whereas the lowest surface area of 279 ± 1.6 $m^2 \cdot g^{-1}$ was found for the untreated zeolite.

The particle size and morphologies of treated and untreated zeolite catalysts were observed by SEM as shown in Figure 4. It can be observed from the SEM images that very tiny particle with unclear shapes, within a few nm size ranges, agglomerate with each other to form irregular clusters with different morphologies. In order to observe the clear morphologies and confirm the mesoporosity of the zeolite catalyst, a high-resolution transmission electron microscopy analysis must be performed. The results indicate that most of the crystals keep their shapes after treatments. However, some surface roughness was observed in the SEM images. These results match well with the results of the literature [27].

Table 3. N_2 adsorption-desorption isotherms of untreated and treated zeolites.

Catalysts	S_{BET} * ($m^2 \cdot g^{-1}$)	V_p ** ($mL \cdot g^{-1}$)	D_p *** (nm)	t-Plot Values	
				External Surface Area ($m^2 \cdot g^{-1}$)	$V_{Micropore}$ ($cm^3 \cdot g^{-1}$)
ZSM-5	279 ± 1.6	0.18	1.7 ± 0.1	55	0.13
ZSM-5-Na	328 ± 1.2	0.26	3.7 ± 0.1	65	0.08
ZSM-5-T	390 ± 1.9	0.23	11.1 ± 0.1	60	0.12
ZSM-5-C	395 ± 2.5	0.37	14.9 ± 0.1	300	0.06
ZSM5-CT	419 ± 2.0	0.34	15.2 ± 0.1	200	0.08

* S_{BET}: BET surface area estimated using 0.05–0.3 relative pressure range; ** V_p: total pore volume ($mL \cdot g^{-1}$) was calculated at P/P_o = 0.99; *** D_p: mean pore size (nm) estimated by using the BJH model from N_2 desorption isotherm.

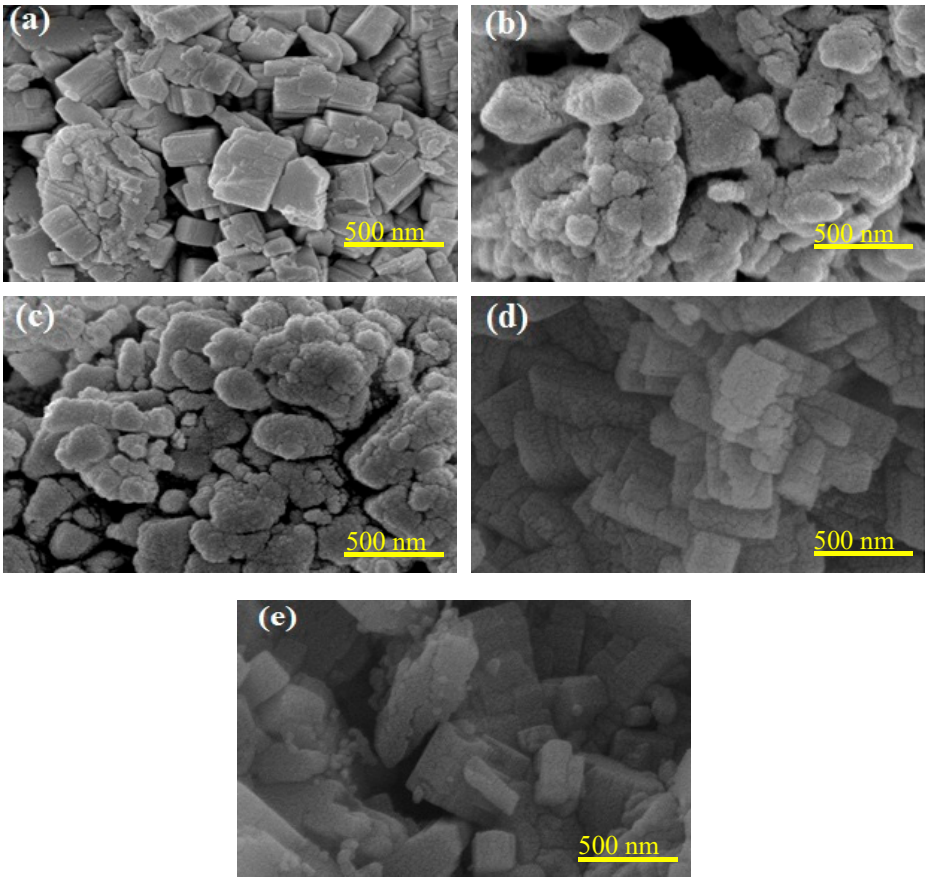

Figure 4. SEM images for (**a**) ZSM-5, (**b**) ZSM-5-Na, (**c**) ZSM-5-C, (**d**) ZSM-5-T and (**e**) ZSM-5-CT.

3.2. Catalytic Performance

The reaction of anisole and propionic anhydride was conducted with untreated zeolite (parent ZSM-5) and treated zeolite catalysts (ZSM-5-Na, ZSM-5-T, ZSM-5-C, and ZSM-5-CT) as shown in Scheme 1. The main product obtained in this acylation reaction was p-methoxypropiophenone. It was found that the untreated zeolite and treated zeolites showed selective characteristic towards para orientation isomer instead of other orientation (ortho and meta) isomers because of its smaller molecular sizes in comparison to its counterpart ortho or meta position isomers. This agrees with other reported studies on the selectivity of zeolite catalysts towards the para position for many instances of aromatic acylation [28,29]. The anisole conversion was found to be 40, 56, 76, 88, and 90%, with the product selectivity toward p-methoxypropiophenone being 60, 66, 83, 94 and 96%, respectively. This revealed that the amount of anisole conversion increases with the increasing BET surface area and

average pore size. In addition, the surface acidity of the zeolite catalysts may have an important role in anisole's high conversion with more selectivity towards the product. Figure 5 shows two resulting peaks that correlated to the two different types of active acid sites. The high-temperature peak was attributed to the desorption of ammonia from strong Brønsted and Lewis acidic sites [30]. Furthermore, the low-temperature peak was attributed to ammonia weakly held or physically adsorbed on the zeolite, which might be due to the desorption of weakly adsorbed NH_3 on weak acidic or non-acidic sites [31], the weak Brønsted acidic sites [32], the Lewis acidic sites [33]; or the silanol groups [30]. The NH_3-TPD results confirmed that the untreated zeolite catalyst possesses low acidic properties in comparison with the treated zeolite catalysts.

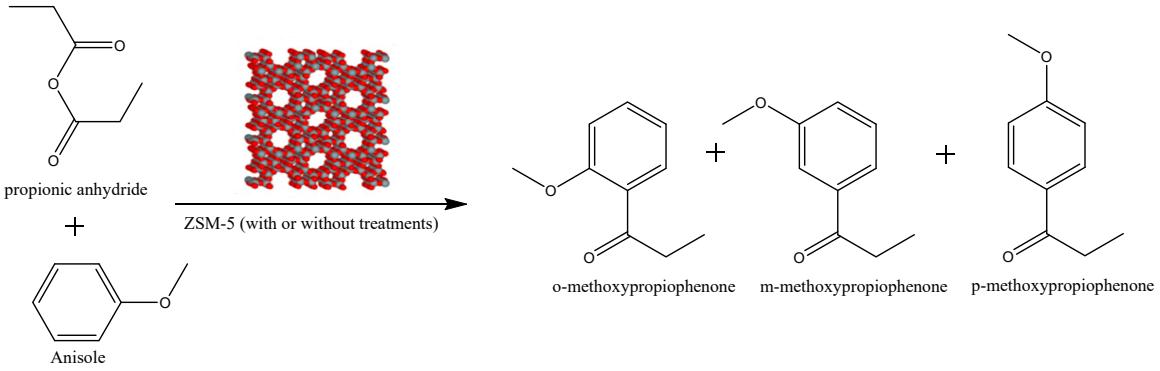

Scheme 1. Reaction pathway for Friedel-Crafts acylation of anisole and propionic anhydride.

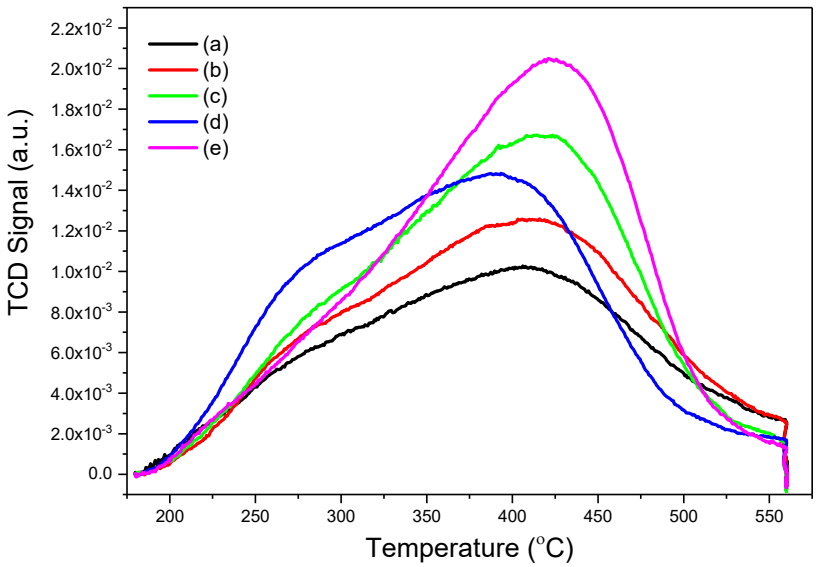

Figure 5. NH_3-TPD profiles of (**a**) ZSM-5, (**b**) ZSM-5-Na, (**c**) ZSM-5-T, (**d**) ZSM-5-C and (**e**) ZSM-5-CT.

Table 4 summarizes the results obtained from the NH_3-TPD measurements. It has been found that the treated zeolite catalyst with a mixed surfactant template to form ZSM-5-CT is the most active form in the Friedel-Crafts acylation reaction of anisole with propionic anhydride, giving 90% conversion and 96% selectivity toward p-methoxypropiophenone. The effect of reaction temperatures of 60, 80, 100, and 120 °C on the acylation of anisole was also studied over untreated and treated zeolite catalysts for 24 h. It can be observed from Figure 6 that anisole conversion and p-methoxypropiophenone selectivity increased by increasing the reaction temperature up to 100 °C, then with a further in temperature up to 120 °C there were slight decreases in conversion and selectivity. This might be because of the inhibiting effect of p-methoxypropiophenone which can be strongly adsorbed on the catalyst at higher conversion rates [34]. In this work, the highest conversion and the best selectivity using the ZSM-5-CT

catalyst were found to be at 100 °C in order to reach 90% of conversion and 96% for selectivity. The overall results of conversion%, yield%, and selectivity% are presented in Table 5. Further investigations on the mechanism of this reaction could be carried out and compared with the literature [35,36] in a future publication.

Table 4. Determination of total acidity of untreated and treated zeolites using NH_3-TPD analysis.

Catalyst	Desorbed NH_3 Amount (mmol·g^{-1})			T_{max} (°C)	
	First Peak	Second Peak	Total	First Peak	Second Peak
ZSM-5	0.45	0.49	0.94	304	422
ZSM-5-Na	0.46	0.53	0.99	306	423
ZSM-5-T	0.74	0.49	1.23	331	426
ZSM-5-C	0.44	0.84	1.28	284	388
ZSM-5-CT	0.47	0.86	1.33	332	427

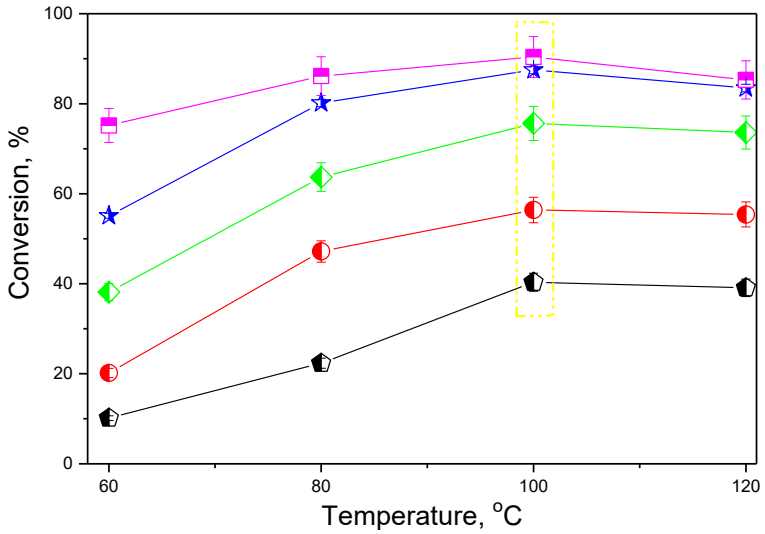

Figure 6. Effect of reaction temperature on the percentage of anisole conversion over treated and untreated zeolite catalysts. Untreated zeolite (ZSM-5) is in black, ZSM-5-NA is in red, ZSM-5-T is in green, ZSM-5-C is in blue, and ZSM-5-CT is in purple.

Table 5. The percentages of conversion, selectivity, and yield for Friedel-Crafts acylation of anisole and propionic anhydride catalyzed by untreated and treated zeolites at 24 h and 100 °C.

Catalyst Code	Conversion (%)	Selectivity (%)	Yield (%)
ZSM-5	40	60	24
ZSM-5-Na	56	66	37
ZSM-5-T	76	83	63
ZSM-5-C	88	94	82
ZSM-5-CT	90	96	87

4. Conclusions

Meso-porous ZSM-5 catalysts have been synthesized for the Friedel-Crafts acylation reaction of anisole and propionic anhydride to obtain p-methoxypropiophenone. The ZSM-5-CT proved to be an active catalyst for this reaction at 100 °C and 24 h. The activity of ZSM-5-CT enhanced selectivity toward the main product by a factor of 1.7 or higher compared to untreated zeolite owing to an increase in surface area and surface acidity.

90% conversion and 96% product selectivity toward p-methoxypropiophenone was achieved by using the ZSM-5-CT catalyst. The catalytic activity depends on the acid strength, number of Brønsted

acidic sites, surface area, average pore size and mesoporosity of the treated zeolite catalysts. The effect of treatment on the zeolite (ZSM-5) catalyst with NaOH, CTABr, and TPAOH and a mixture of solutions (CTAB + TPAOH) solutions were studied.

Author Contributions: Investigation and formal analysis, H.A.S.; conceptualization and supervision, K.M.S. and Z.R.; writing—original draft, H.A.S. and J.G.; proofreading and editing, M.R., A.-S.N. and J.G.; reviewing and final editing, J.G.; funding acquisition, K.M.S.

Acknowledgments: The authors are grateful to the Salahaddin University-Erbil (SUE) in Kurdistan Regional Government (KRG) for financial support.

Conflicts of Interest: The authors declare no conflict of interest.

References

1. Olah, G.A.; Donovan, D.J.; Lin, H.C. Friedel-Crafts Chemistry. 1. *Chem. Informationsdienst* **1976**, *98*, 2661–2663.
2. Clark, J.H. Solid acids for green chemistry. *Acc. Chem. Res.* **2002**, *35*, 791–797. [CrossRef] [PubMed]
3. Corma, A.; JoséCliment, M.; García, H.; Primo, J. Design of synthetic zeolites as catalysts in organic reactions: Acylation of anisole by acyl chlorides or carboxylic acids over acid zeolites. *Appl. Catal.* **1989**, *49*, 109–123. [CrossRef]
4. Gaare, K.; Akporiaye, D. Modified zeolites as catalysts in the Friedel-Crafts acylation. *J. Mol. Catal. A Chem.* **1996**, *109*, 177–187. [CrossRef]
5. Freese, U.; Heinrich, F.; Roessner, F. Acylation of aromatic compounds on H-Beta zeolites. *Catal. Today* **1999**, *49*, 237–244. [CrossRef]
6. Smith, K.; Zhenhua, Z.; Hodgson, P.K. Synthesis of aromatic ketones by acylation of aryl ethers with carboxylic anhydrides in the presence of zeolite H-β (H-BEA) in the absence of solvent. *J. Mol. Catal. A Chem.* **1998**, *134*, 121–128. [CrossRef]
7. Ma, Y.; Wang, Q.; Jiang, W.; Zuo, B. Friedal-Crafts acylation of anisole over zeolite catalysts. *Appl. Catal. A Gen.* **1997**, *165*, 199–206. [CrossRef]
8. Selkirk, J.; Challiss, R.; Price, G.; Nahorski, S. Differential coupling to endogenous G protein subpopulations in CHO and BHK cell lines recombinantly expressing mGlu1 receptors. *Br. J. Pharmacol.* **1999**, *128*, 32.
9. Zaarour, M.; Dong, B.; Naydenova, I.; Retoux, R.; Mintova, S. Progress in zeolite synthesis promotes advanced applications. *Microporous Mesoporous Mater.* **2014**, *189*, 11–21. [CrossRef]
10. Choi, M.; Na, K.; Kim, J.; Sakamoto, Y.; Terasaki, O.; Ryoo, R. Stable single-unit-cell nanosheets of zeolite MFI as active and long-lived catalysts. *Nature* **2009**, *461*, 246–249. [CrossRef] [PubMed]
11. Petushkov, A.; Yoon, S.; Larsen, S.C. Synthesis of hierarchical nanocrystalline ZSM-5 with controlled particle size and mesoporosity. *Microporous Mesoporous Mater.* **2011**, *137*, 92–100. [CrossRef]
12. Jin, H.; Ansari, M.B.; Park, S.-E. Mesoporous MFI zeolites by microwave induced assembly between sulfonic acid functionalized MFI zeolite nanoparticles and alkyltrimethylammonium cationic surfactants. *Chem. Commun.* **2011**, *47*, 7482–7484. [CrossRef] [PubMed]
13. Galarneau, A.; Iapichella, J.; Bonhomme, K.; Di Renzo, F.; Kooyman, P.; Terasaki, O.; Fajula, F. Controlling the morphology of mesostructured silicas by pseudomorphic transformation: A route towards applications. *Adv. Funct. Mater.* **2006**, *16*, 1657–1667. [CrossRef]
14. Gonçalves, M.L.; Dimitrov, L.D.; Jordão, M.H.; Wallau, M.; Urquieta-González, E.A. Synthesis of mesoporous ZSM-5 by crystallisation of aged gels in the presence of cetyltrimethylammonium cations. *Catal. Today* **2008**, *133*, 69–79. [CrossRef]
15. Wang, L.; Yin, C.; Shan, Z.; Liu, S.; Du, Y.; Xiao, F.-S. Bread-template synthesis of hierarchical mesoporous ZSM-5 zeolite with hydrothermally stable mesoporosity. *Colloids Surf. A Physicochem. Eng. Asp.* **2009**, *340*, 126–130. [CrossRef]
16. Shanbhag, G.V.; Choi, M.; Kim, J.; Ryoo, R. Mesoporous sodalite: A novel, stable solid catalyst for base-catalyzed organic transformations. *J. Catal.* **2009**, *264*, 88–92. [CrossRef]
17. Groen, J.C.; Moulijn, J.A.; Pérez-Ramírez, J. Decoupling mesoporosity formation and acidity modification in ZSM-5 zeolites by sequential desilication-dealumination. *Microporous Mesoporous Mater.* **2005**, *87*, 153–161. [CrossRef]

18. Harding, G. X-ray diffraction imaging—A multi-generational perspective. *Appl. Radiat. Isot.* **2009**, *67*, 287–295. [CrossRef] [PubMed]
19. Gardy, J.; Hassanpour, A.; Lai, X.; Ahmed, M.H. Synthesis of Ti(SO_4)O solid acid nano-catalyst and its application for biodiesel production from used cooking oil. *Appl. Catal. A Gen.* **2016**, *527*, 81–95. [CrossRef]
20. Rusu, D.; Rusu, G.; Luca, D. Structural characteristics and optical properties of thermally oxidized zinc films. *TC* **2011**, *100*, 101. [CrossRef]
21. Gardy, J. Biodiesel Production from Used Cooking Oil Using Novel Solid Acid Catalysts. Ph.D. Thesis, University of Leeds, Leeds, UK, 2017.
22. Byrappa, K.; Kumar, B.S. Characterization of zeolites by infrared spectroscopy. *Asian J. Chem.* **2007**, *19*, 4933.
23. Zhang, Y.; Zhu, K.; Duan, X.; Li, P.; Zhou, X.; Yuan, W. Synthesis of hierarchical ZSM-5 zeolite using CTAB interacting with carboxyl-ended organosilane as a mesotemplate. *RSC Adv.* **2014**, *4*, 14471–14474. [CrossRef]
24. Jash, P.; Meaux, K.; Trenary, M. Transmission infrared spectroscopy of ammonia borane. *J. Undergrad. Res.* **2012**, *5*. [CrossRef]
25. Oh, H.-S.; Kang, K.-K.; Kim, M.-H.; Rhee, H.-K. Synthesis of MFI-type zeolites under atmospheric pressure. *Korean J. Chem. Eng.* **2001**, *18*, 113–119. [CrossRef]
26. Kresge, C.; Leonowicz, M.; Roth, W.; Vartuli, J.; Beck, J. Ordered mesoporous molecular sieves synthesized by a liquid-crystal template mechanism. *Nature* **1992**, *359*, 710–712. [CrossRef]
27. Wang, B. Zeolite Deactivation during Hydrocarbon Reactions: Characterisation of Coke Precursors and Acidity, Product Distribution. Ph.D. Thesis, UCL (University College London), London, UK, 2008.
28. Chiche, B.; Finiels, A.; Gauthier, C.; Geneste, P.; Graille, J.; Pioch, D. Friedel-Crafts acylation of toluene and p-xylene with carboxylic acids catalyzed by zeolites. *J. Organ. Chem.* **1986**, *51*, 2128–2130. [CrossRef]
29. Chiche, B.; Finiels, A.; Gauthier, C.; Geneste, P. The effect of structure on reactivity in zeolite catalyzed acylation of aromatic compounds: A ρ-σ+ relationship. *Appl. Catal.* **1987**, *30*, 365–369. [CrossRef]
30. Topsøe, N.-Y.; Pedersen, K.; Derouane, E.G. Infrared and temperature-programmed desorption study of the acidic properties of ZSM-5-type zeolites. *J. Catal.* **1981**, *70*, 41–52. [CrossRef]
31. Tsiatouras, V.A.; Evmiridis, N.P. Study of interactions between ion-exchanged chromium and impregnated vanadium in USY zeolite material. *Ind. Eng. Chem. Res.* **2003**, *42*, 1137–1144. [CrossRef]
32. Hidalgo, C.V.; Itoh, H.; Hattori, T.; Niwa, M.; Murakami, Y. Measurement of the acidity of various zeolites by temperature-programmed desorption of ammonia. *J. Catal.* **1984**, *85*, 362–369. [CrossRef]
33. Karge, H.G. Comparative measurements on acidity of zeolites. *Stud. Surf. Sci. Catal.* **1991**, *65*, 133–156.
34. Botella, P.; Corma, A.; Lopez-Nieto, J.; Valencia, S.; Jacquot, R. Acylation of toluene with acetic anhydride over beta zeolites: Influence of reaction conditions and physicochemical properties of the catalyst. *J. Catal.* **2000**, *195*, 161–168. [CrossRef]
35. Ramanathan, A.; Zhu, H.; Maheswari, R.; Subramaniam, B. Novel zirconium containing cage type silicate (Zr-KIT-5): An efficient Friedel-Crafts alkylation catalyst. *Chem. Eng. J.* **2015**, *278*, 113–121. [CrossRef]
36. Cirujano, F.G.; Stalpaert, M.; De Vos, D.E. Ionic liquids vs. microporous solids as reusable reaction media for the catalytic C–H functionalization of indoles with alcohols. *Green Chem.* **2018**, *20*, 2481–2485. [CrossRef]